Biochimica et Biophysica Acta, 465 (1977) 535—549

BBA 77630

THE INVOLVEMENT OF SARCOTUBULAR MEMBRANES IN GENETIC MUSCULAR DYSTROPHY

D. SCALES, R. SABBADINI and G. INESI

Laboratory of Physiology and Biophysics, University of the Pacific, San Francisco, Calif., 94115 (U.S.A.)

(Received August 23rd, 1976)

Summary

Microsomal preparations from breast muscle of normal and dystrophic chickens are characterized with regard to ultrastructural features, protein composition, Ca^{2+} transport and ATPase activity.

Dystrophic muscle yields a greater microsomal dry weight, with a reduced protein to lipid ratio. This is related to the presence of a considerable number of low density microsomes, in addition to seemingly normal microsomes. The low density microsomes display a reduced number of protein particles on freeze fracture faces.

Electrophoretic analysis reveals nearly identical patterns in normal and dystrophic microsomes. Furthermore, normal and dystrophic microsomes sustain equal rates of Ca^{2+} transport and ATPase, demonstrating an identical protein specific activity. However, the dystrophic microsomes have a lower capacity to retain transported Ca^{2+}.

The high yield of low density microsomes with reduced capacity for Ca^{2+} uptake is attributed to the presence of membranes proliferated in the junctional and tubular sarcomere regions of the dystrophic muscle. It is suggested that proliferation of such membranes accounts for the altered excitation-contraction coupling and cable properties of genetically dystrophic muscle.

Introduction

Alterations in the contractile behavior of dystrophic muscle have been well documented [1—5]. However, such alterations do not appear to be accompanied by abnormalities of the contractile proteins [6—10]. This suggests that

Abbreviations: EGTA, ethyleneglycol bis (β-aminoethylether)-*N*,*N*'-tetraacetic acid; MOPS, morpholinopropane sulfonic acid.

deranged excitation-contraction coupling may be responsible for the observed contractile behavior. In fact, abnormalities of Ca^{2+} transport were observed in muscle microsomes isolated from dystrophic animal models [9—17] and humans [18,20].

With the present work we have characterized microsomes prepared from breast muscle of normal and dystrophic chicken, with regard to structural and functional features. We have found that microsomal preparations from dystrophic muscle contain a large number of microsomes originating from membranes proliferated in the junctional and tubular regions of the sarcomere. These microsomes have a reduced capacity to retain transported calcium.

Methods

Normal (line 412) and dystrophic (line 413) chickens were obtained from the University of California at Davis (Department of Avian Sciences) and sacrificed at 5—6 weeks of age.

Microsomes were prepared by homogenizing in a Warring blender 100 g of breast muscle in 300 ml of 10 mM morpholinopropane sulfonic acid (MOPS) pH 6.8 and 10% sucrose. The homogenization was carried out for 15 s every 5 min for 1 h. During this time the pH was maintained at pH 6.8 by occasional addition of a few drops of 5% NaOH. The consistency of the homogenization procedure was found necessary to obtain a reproducible yield and a low ionic strength homogenization medium was used in order to minimize extraction of contractile proteins.

Following homogenization, centrifugation was carried out for 20 min at 15 000 × *g*. The supernatant was then collected and filtered through gauze to remove floating particles. A second centrifugation was then carried out for 90 min at 40 000 × *g*. This supernatant was discarded and the sediment dissolved in 10 mM MOPS pH 6.8 and 0.6 M KCl. After 1 h incubation for extraction of contractile proteins, a centrifugation at 15 000 × *g* for 20 min was carried out. The supernatant was then centrifuged at 40 000 × *g* for 90 min. The sediment was suspended in 10 mM MOPS pH 6.8 and 28% sucrose at an approximate protein concentration of 10 mg/ml. This suspension is referred to as "standard" preparation.

The standard preparation was further divided in fractions of different densities by centrifugation in sucrose gradients (28—43% sucrose, 10 mM MOPS pH 6.8) for 20 h at 68 000 × *g* in a Beckman SW-41 swinging bucket rotor. All preparation procedures were carried out at 2° C.

Microsomal dry weight was determined after repeated washings in distilled water and drying in vacuum until constant weight was reached. A Mettler microbalance was used for these determinations. Total protein was measured with the biuret or Folin reagents, standardized by Kjeldahl nitrogen determinations. Electrophoretic analysis of solubilized membrane proteins was performed as previously described [21]. Calcium transport measurements were made by isotopic distribution methods [22] and confirmed by parallel experiments with metallochromic indicators [17].

ATPase activity was determined by following the liberation of inorganic phosphate [23]. Negative staining and freeze fracture preparations [24] or

microsomes for electronmicroscopy were made as previously described [21].

Samples of pectoralis muscle were excised and prepared for thin sectioning and freeze fracturing as described earlier [24]. Thin sections were prepared as follows: small pieces of the muscle were fixed in 4% glutaraldehyde in Millonig's buffer (pH 7.3) for 1 h and then washed in buffer. Then they were post-fixed in 2% osmium tetroxide for 1 h, dehydrated and embedded. Sections were cut on a Porter Blum MT-2 and then stained with uranyl acetate and lead citrate.

Other pieces of the muscle were fixed for 15 min in phosphate-buffered saline (pH 7.4), washed several times and then glycerol was added gradually until the concentration reached 20%. They were incubated for 1 h before freezing in liquid Freon 22 and then fractured at −100°C and replicated in a Balzers freeze fracturing device (EM Laboratory, University of California at Berkeley).

All thin sections and freeze fracture replicas were examined in a Philips EM 200 at 80 kV.

Results and Discussion

Yield of microsomes

An important part of our studies was a quantitation of microsomal yield in terms of dry weight, protein and total lipids. As shown in Table I, we found that in standard preparations the yield of microsomal dry weight from dystrophic muscle was approximately twice that obtained from normal muscle. This difference was mostly due to an increase in total lipid content as reflected by the lower protein to lipid ratio found in dystrophic as compared to normal microsomes.

Prolonged sucrose gradient centrifugation resolved standard microsomal preparations into two distinct bands (S_1 and S_2 in Fig. 1) sedimenting between 28 and 32% and 32 and 39% sucrose respectively. An additional diffuse fraction (S_3) sedimented between 39 and 43% sucrose. It is apparent in Fig. 1 that the high lipid content of the preparations obtained from dystrophic muscle is reflected in a greater yield of light (S_1) microsomes.

Electrophoretic analysis (Fig. 2) of solubilized microsomes revealed a pattern with one prominent protein component of approximately 100 000 mol.

TABLE I

YIELD ESTIMATES AND PROTEIN/LIPID RATIOS

Values are means ± 2 S.E.M. (n = 8).

	Microsomal yield (mg protein/g wet wt.)	Protein/lipid ratio (mg/mg)	Dry weight yield (mg/g wet wt.)
Normal	0.578 ±0.114	2.03 ±0.08	0.851
Dystrophic	0.832 ±0.171	1.23 ±0.375	1.85
Dystrophic/normal (× 100)	144	60	216
P value	<0.01	<0.01	—

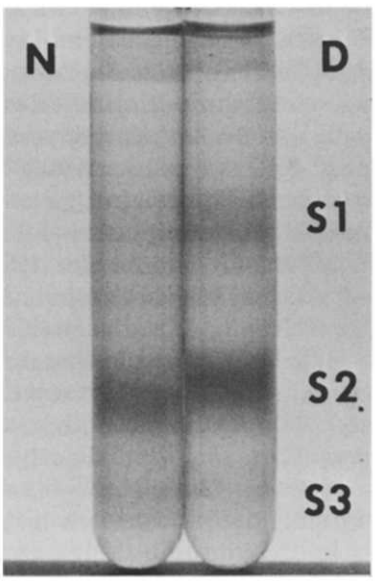

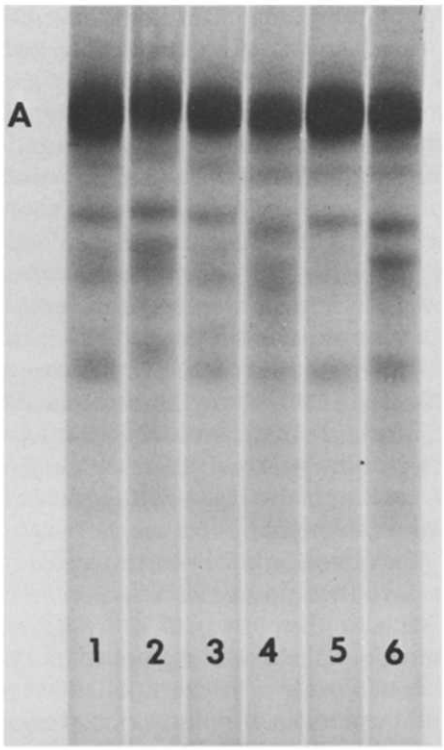

Fig. 1. The appearance of normal (N) and dystrophic (D) microsomes after centrifugation on discontinuous sucrose gradients (28—43% sucrose) for 20 h at 68 000 g. The microsomes form two distinct bands (S_1 and S_2) and one diffuse band (S_3).

Fig. 2. Polyacrulamide gel electrophoresis of microsomal protein (25—30 μg per gel). The protein was solubilized in 1% SDS. The 106 000 dalton calcium-ATPase (A) represents over 75% of the total protein. The numbers refer to the following microsomal preparations: (1) normal standard preparation; (2) dystrophic standard preparation; (3) normal S_1; (4) dystrophic S_1; (5) normal S_2; (6) dystrophic S_2.

wt., which was previously identified with the ATPase enzyme [25—27]. Although other minor protein components were also present, the electrophoretic pattern remained essentially identical when standard preparations and sucrose gradient fractions of either normal or dystrophic muscle were analyzed.

Structural observations

Electron microscopic inspection of negatively stained microsomes revealed vesicular structures similar to those observed in previous preparations of fragmented sarcoplasmic reticulum [28,29]. Further ultrastructural characterization was then carried out by study of the inner faces of the two membrane leaflets exposed by freeze fracturing [30]. In sarcoplasmic reticulum this technique has revealed the presence of 90 Å particles which have been identified with the ATPase protein [31—33]. In purified rabbit sarcoplasmic reticulum vesicles the protein particles are found mostly associated with the concave faces

TABLE II

FRACTURE FACE DISTRIBUTION

The concave fracture faces were sorted into two classes: P_*, concave faces containing numerous particles; P_0, concave faces containing few or no particles. The fraction or probability of occurrence, p, of each type was determined by counting and sorting 500 normal and 500 dystrophic concave fracture faces. N: normal; D: dystrophic.

	$p(P_*)$	$p(P_0)$
NS_1	0.48	0.52
NS_2	0.89	0.11
DS_1	0.37	0.63
DS_2	0.55	0.45

(cytoplasmic membrane leaflet), while the convex faces (inner leaflet) are mostly smooth.

Freeze fracturing of chicken breast muscle microsomes also revealed an approximately equal number of concave and convex faces, consistent with the origin of the two faces from complementary membrane leaflets. Most of the convex faces were smooth (E_0 faces) and only a small fraction of convex faces contained particles (E_* faces). This fraction appeared to be higher in replicas obtained from dystrophic microsomes.

The concave faces could also be separated in two groups: one with numerous particles (P_* faces) and the other with a low number of particles (P_0 faces). Table II shows that fractionation in sucrose gradient enriched the heavy fraction with vesicles originating P_* faces. A lower percentage of P_* faces was found in all fractions of dystrophic as compared to normal microsomes. This agrees with the fracture face distribution of the standard preparations reported earlier [17]. Fig. 3 shows typical fracture faces observed in the sucrose-purified preparations.

Determinations of particle densities on a large number of concave faces confirmed these conclusions. An example of such determinations is given in Fig. 4, in which the distribution of concave faces as a function of particle density clearly demonstrates the presence of two groups with high (P_*, 2000—4000/μm^2), and low (P_0, 600/μm^2), particle densities. In dystrophic microsomes (Fig. 4B) the separation between the two groups is not as definite and it is apparent that the number of concave faces with low ($<1000/\mu m^2$) and intermediate ($\approx 2000/\mu m^2$) particle densities is much higher than in normal microsomes.

Our observations indicate that the greater yield of microsomal dry weight obtained from dystrophic muscle in accounted for by microsomes with a low and intermediate particle density. This is reflected in the freeze fracture face distribution, as well as in the protein to lipid ratio.

Characterization of microsomes

The nearly identical electrophoretic patterns shown in Fig. 2 indicate that in all fractions of normal and dystrophic microsomes examined in our experiments the predominant protein component migrates with a velocity corresponding to that of sarcoplasmic reticulum ATPase. In separate experiments we determined the electrophoretic patterns of mitochondrial and sarcolemmal

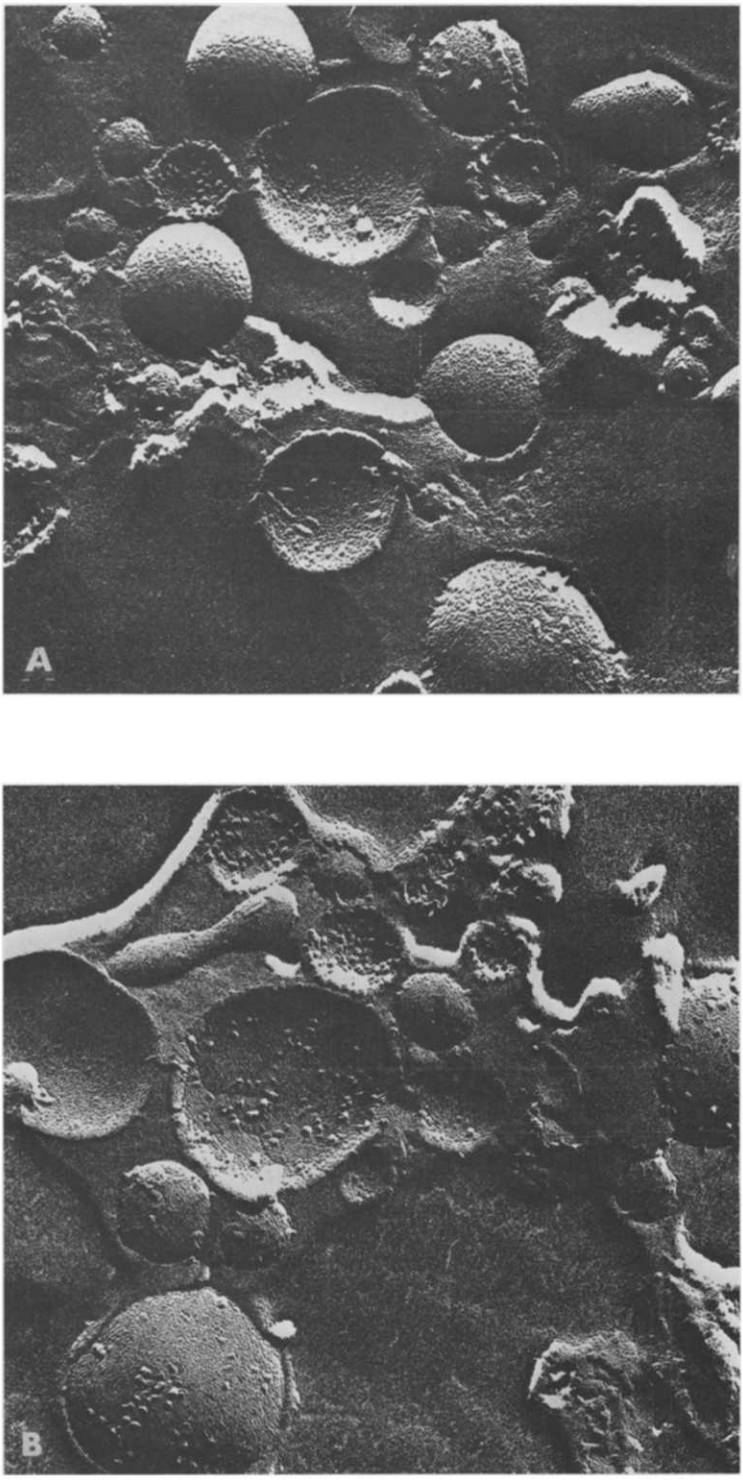

Fig. 3. For legend see opposite page.

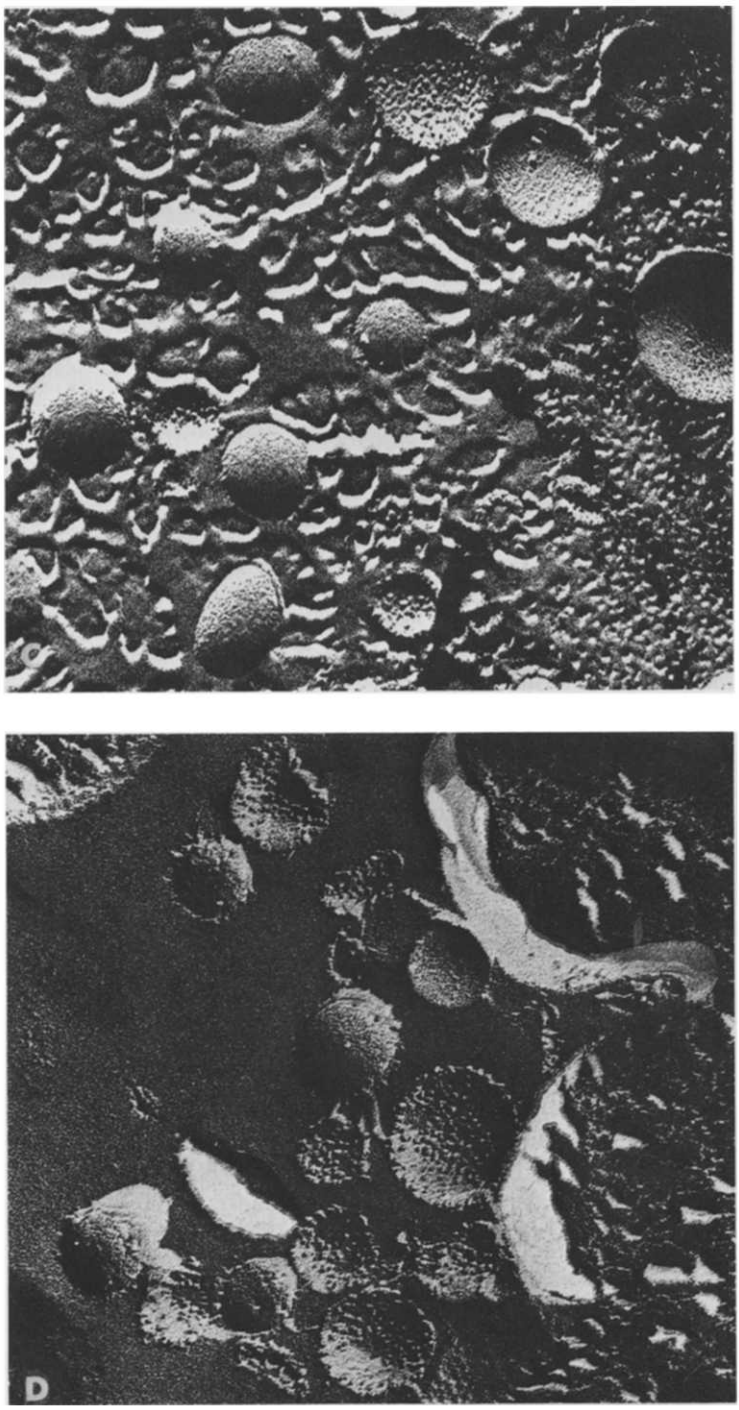

Fig. 3. (A) Freeze fracture replica of the light fraction of dystrophic microsomes (DS_1). (B) The heavy fraction of dystrophic microsomes (DS_2). (C) The light fraction of normal microsomes (NS_1). (D) The heavy fraction of normal microsomes (NS_2). All micrographs shown at × 99 000. These micrographs were selected to show the distribution of fracture face types as discussed in the text. By themselves they do not accurately reflect the distribution shown in Table II since they represent only a small part of the total area examined. Note the larger diameter of the dystrophic fracture faces, which is consistent with their origins from swollen sarcotubular elements.

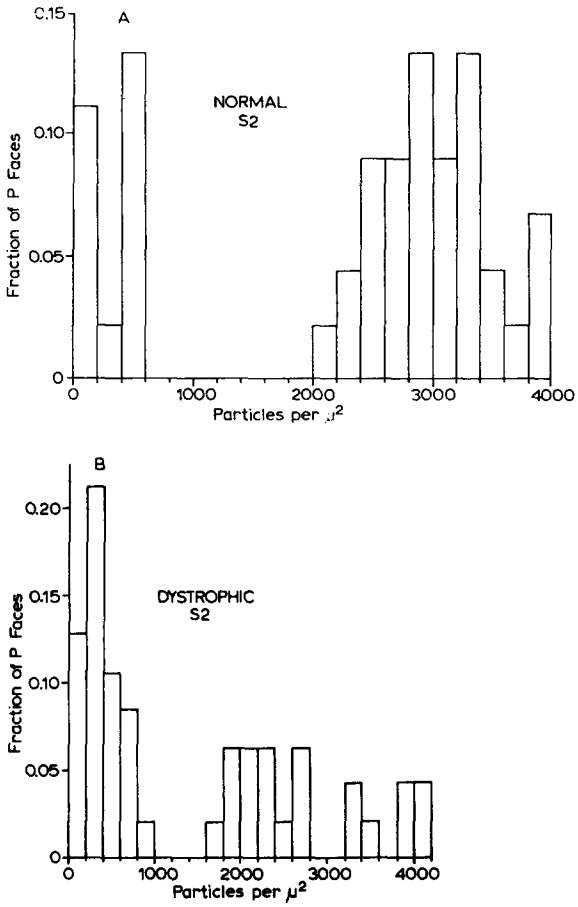

Fig. 4. (A) The distribution of concave fracture faces observed in the heavy fraction (S_2) of normal microsomes. (B) The distribution for the heavy fraction of dystrophic microsomes. Particle densities were estimated for over 100 concave faces from four different preparations.

membrane fractions and we found no significant cross contaminations of those fractions with our microsomes. This is in agreement with the identical levels of specific ATPase activity found in the various microsomal fractions (see below) and with the absence of significant levels of mitochondrial (azide sensitive) and ($Na^+ + K^+$)-ATPase activities. These observations suggest that the chicken breast microsomes originate mostly from sarcotubular membranes.

It is known, however, that the particle distribution in freeze fracture preparations of whole muscle is not homogenous in the various regions of the sarcotubular system within the sarcomere, and at least two regions of sarcoplasmic reticulum have been distinguished based on this observation: junctional sarcoplasmic reticulum (at dyads or triads) and longitudinal sarcoplasmic reticulum (elsewhere) [34].

Our observations of freeze fractured dystrophic chicken pectoralis muscle agree qualitatively with these findings from other species and are shown in Fig. 5. The particles on the *P* face of junctional sarcoplasmic reticulum (i.e., at the

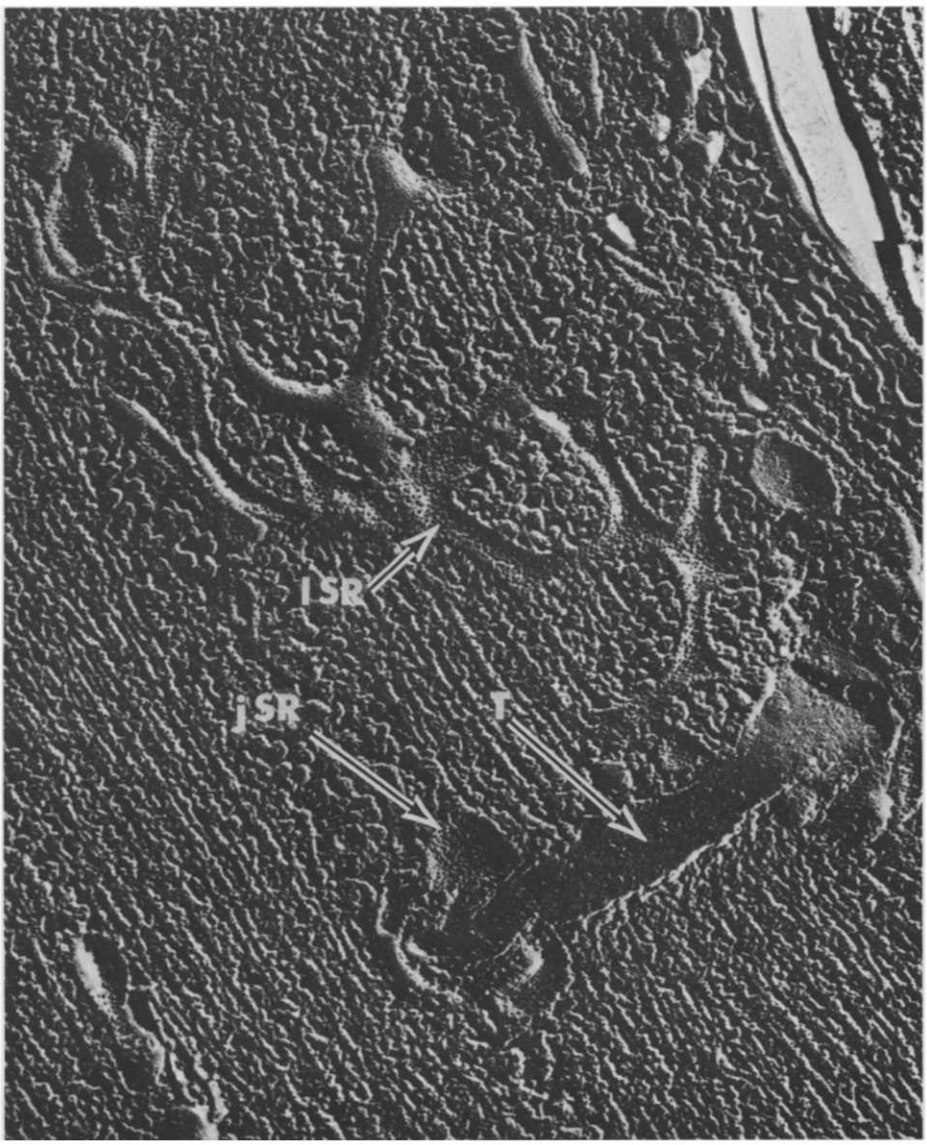

Fig. 5. A freeze fracture replica of dystrophic muscle showing the system of sarcotubular membranes. Across the bottom and transverse to the fiber axis is the *P* face of a *T* tubule showing a low particle density of about 300/μm^2. Surrounding the left end of the T tubule are *P* face elements of the terminal cisternae or junctional sarcoplasmic reticulum (j SR) with a particle density of 2500/μm^2. Extending above the right end of the T tubule is an anastomosing fragment of the *P* face of longitudinal sarcoplasmic reticulum (lSR) (3700 particles/μm^2), which cross fractures near the top to reveal the smooth *E* face × 61 300.

terminal cisternae) are less numerous than the tightly packed particles on the *P* face of the longitudinal elements. The junctional sarcoplasmic reticulum contains particles with an approximate density of 2500/μm^2 whereas the longitudinal sarcoplasmic reticulum contains about 3700/μm^2. The *P* faces of the T

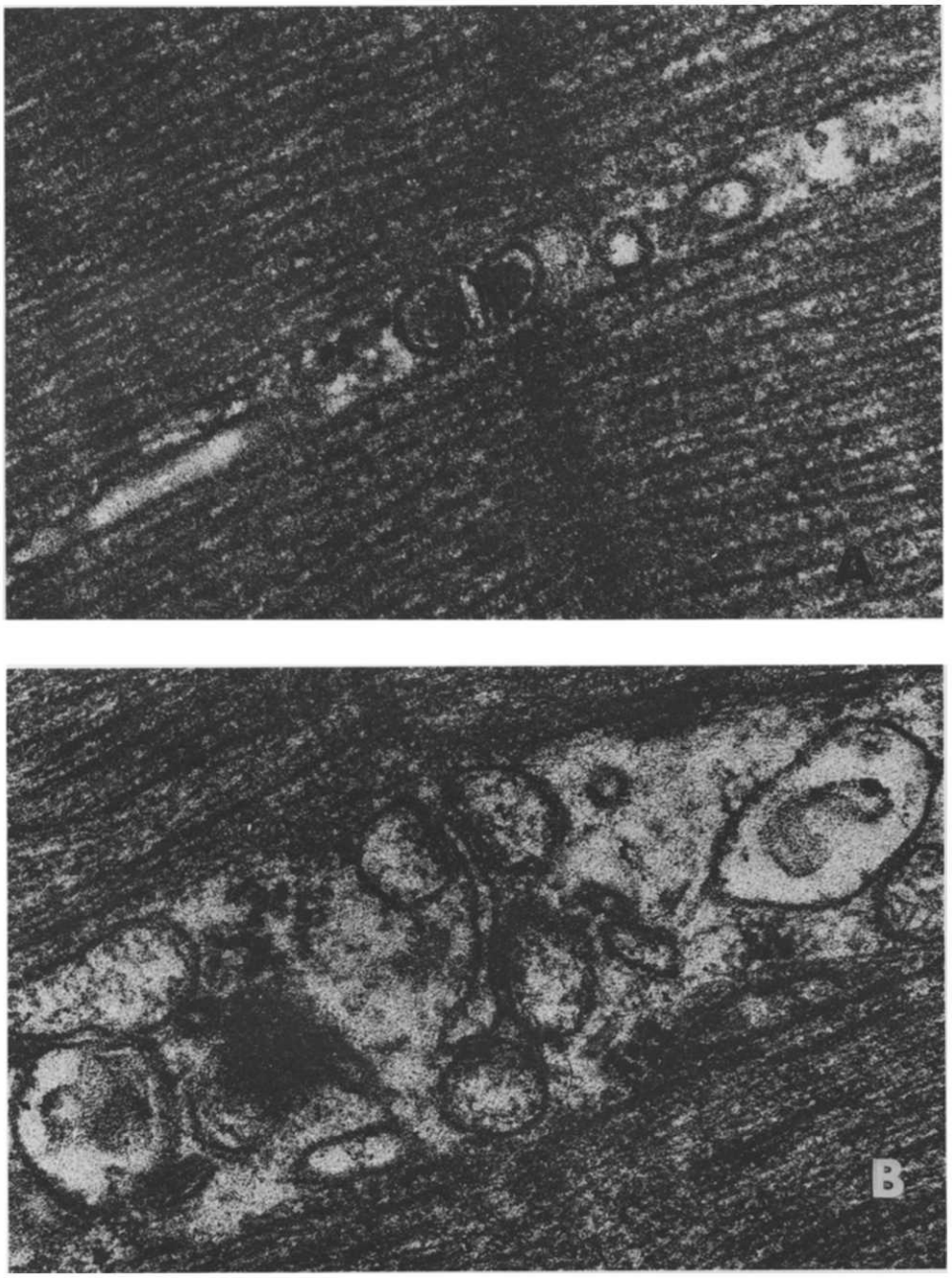

Fig. 6. (A) Longitudinal thin sections of chicken pectoralis muscle show the typical appearance of a normal coupling between a T tubule and juctional sarcoplasmic reticulum (triad). Roughly circular sacs are in close apposition to a flattened tube near the Z line. These sacs contain electron dense material. Junctional feet extend between the sacs and the tube. × 92 000. (B) A similar section of dystrophic muscle shows a disfigured coupling near the Z line. There are typically 4 or 5 sacs containing electron dense material that surround a more elongated and flattened tube. Junctional feet are also visible. The most striking feature of the dystrophic "triad" is that it is not always a triad. The extra sacs of junctional sarcoplasmic reticulum suggest a proliferation of the terminal cisternae, and the larger perimeter of the T tubule also suggests a proliferation of T system membranes in dystrophic muscle. × 92 000.

tubules show a much less dense population of particles than the sarcoplasmic reticulum. Here we find a density of only about $300/\mu m^2$.

A comparison of the ultrastructural observations made on microsomes and on whole muscle suggest that microsomes originating *P* faces with high, intermediate and low particle densities derive from longitudinal, junctional and tubular membranes, respectively. It appears then that normal microsomes consist mostly of longitudinal sarcoplasmic reticulum membrane, while a considerable number of dystrophic microsomes consist of junctional and tubular membranes. This is in agreement with the morphologic appearance of dystrophic muscle in thin sections, showing both an expansion of T tubules and a proliferation of junctional sarcoplasmic reticulum (cf. Figs. 6A and B).

An intriguing question is whether one should expect tubular membranes to have a protein composition similar to sarcoplasmic reticulum membranes or rather to sarcolemmal membranes. The relative contributions to the total protein given by the P_* vs. P_0 and E_* faces was estimated from measurements of protein particle densities and fracture face distributions. These estimates show that the protein accounted for by the dystrophic P_0 and E_* fracture faces was up to 40% of the total protein. Such a large fraction of the total protein would be sufficient to originate distinct electrophoretic and enzymatic patterns. However, our analysis revealed a homogenous protein composition of all microsomal preparations (Fig. 2) with no difference in contaminating (non-sarcoplasmic reticulum) proteins. Therefore, the major protein component of the P_0 and E_* faces has a molecular weight of approx. 100 000 and may in fact represent calcium-ATPase protein.

Functional studies

The main functional feature of sarcoplasmic reticulum membrane vesicles is an ATP dependent Ca^{2+} uptake. On addition of ATP Ca^{2+} is rapidly taken up and maximal calcium levels in the vesicles are reached within 30—60 s. We found these levels to be 125 nmol/mg protein in standard preparations of normal microsomes, while only 65 nmol/mg protein were taken up by dystrophic microsomes (Fig. 7). It is interesting to notice that for both normal and dystrophic microsomes the levels of calcium uptake are lower in the light than in the heavy fractions (Fig. 8). These findings suggest that the deficiency in calcium loading capacity is related to the presence of microsomes with intermediate and low particle density which are found in greater number in the light as compared to the heavier fractions, and in the preparations of dystrophic as compared to normal microsomes.

It was first discovered by Hasselbach and Makinose [35] that in the presence of oxalate the burst of ATP dependent Ca^{2+} uptake is prolonged and the activity proceeds linearly for a considerable time. This effect is attributed to formation of calcium oxalate insoluble product and reduction of the Ca^{2+} activity inside the vesicles.

Under these conditions we found the rates of Ca^{2+} transport by dystrophic microsomes to be at least equal, and in most cases slightly higher than those of normal microsomes (Table III). Analogous results were found with regard to the ATPase activity coupled to calcium transport.

Linear rates of ATPase activity may be obtained even in the absence of

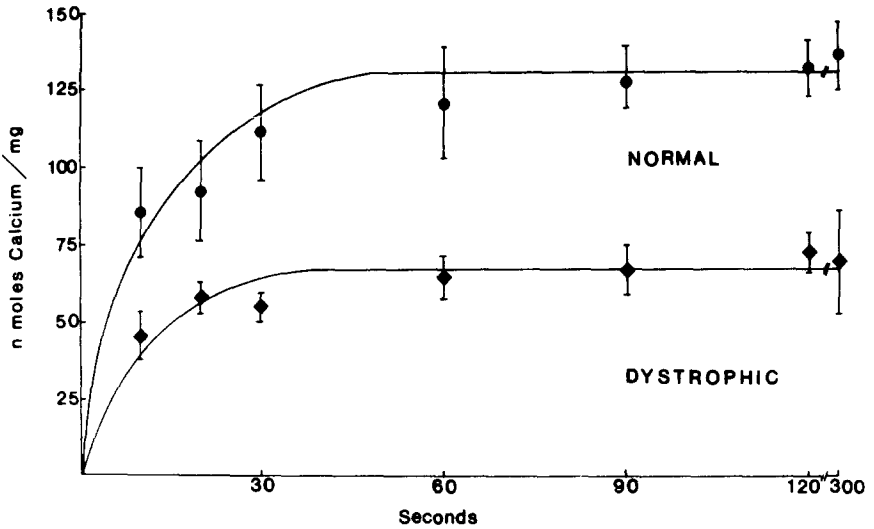

Fig. 7. Calcium uptake curves obtained from standard preparations of microsomes from normal and dystrophic breast muscle. The reaction mixture contained: 20 mM MOPS pH 6.8, 5 mM $MgCl_2$, 100 mM KCl, 0.1 mM EGTA, 0.1 mM $^{45}CaCl_2$, 0.2 mg protein/ml. 25°C. Values are means ± 2 S.E.M. (n = 8).

oxalate, if a detergent such as Triton X-100 is present in the reaction mixture. In this case, solubilization of the membrane structural components prevents the formation of transmembrane Ca^{2+} gradients; therefore, the ATPase activity coupled to Ca^{2+} transport continues linearly as long as substrate is available. In agreement with the measurements made in the presence of oxalate, the Triton-stimulated ATPase is catalyzed at similar rates in normal and dystrophic microsomes [17].

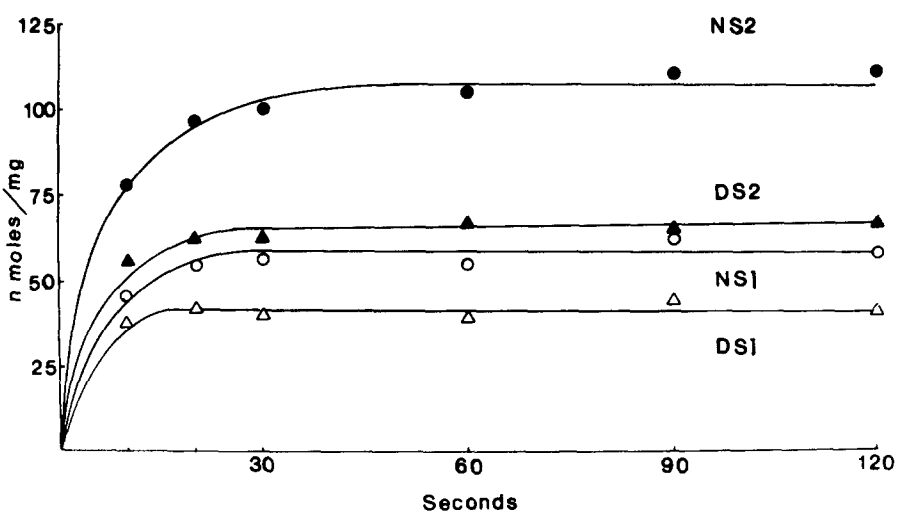

Fig. 8. Calcium uptake curves characteristic of sucrose gradient microsomes. Only the normal (N) and dystrophic (D) light (S_1) and heavy (S_2) fractions are shown. Values for the S_3 fraction were nearly identical to the S_2 values displayed here and are therefore not shown. The reaction mixture was the same as in Fig. 7.

TABLE III

CALCIUM UPTAKE AND ATPase RATES

Reaction mixture contained: 20 mM MOPS pH 6.8, 2 mM $CaCl_2$, 5 mM $MgCl_2$, 2 mM EGTA, 10 mM oxalate, 80 mM KCl, and 0.2 mg/ml protein, 37° C. For measurements of basic ATPase activity, $CaCl_2$ was omitted. Rates were determined from linear regression line analysis of 8 points taken within the first minute. Values are means ± 2 S.E.M. (n = 6). N.S., not significant at the P = 0.05 level.

	Calcium uptake rate (μmol Ca^{2+}/ mg per min)	ATPase rate (μmol P_i/mg per min)		
		Total ((Ca^{2+} + Mg^{2+})-activated)	Basic (Mg^{2+}-activated)	Extra (Ca^{2+}-activated)
Normal	1.45 ±0.52	3.04 ±0.44	1.31 ±0.24	1.73 ±0.16
Dystrophic	2.35 ±0.608	3.15 ±0.488	0.98 ±0.232	2.16 ±0.394
Dystrophic/normal (X100)	162	104	76	125
P value	N.S.	N.S.	N.S.	N.S.

It should be pointed out that all functional parameters are related to protein unit weight and, therefore, express protein (rather than dry weight) specific activity.

Our functional studies, in agreement with the electrophoretic analysis, indicate that the prevalent protein component of normal and dystrophic microsomes is the Ca^{2+}-sensitive ATPase coupled to Ca^{2+} transport. This "pump" protein functions equally well in normal and in dystrophic microsomes. However, the maximal levels of transported calcium retained in the absence of oxalate are lower in the dystrophic than in normal microsomes.

The reduced capacity of dystrophic microsomes to retain calcium could be explained by an increase in their permeability. The efflux of calcium from passively and actively loaded microsomes is currently being investigated in our laboratory. However, preliminary measurements indicate that the kinetics of calcium efflux from dystrophic microsomes do not differ markedly from the normal and therefore cannot account for the reduced calcium loading capacity.

Conclusions

The swelling of intracellular membrane components, most notably mitochondria and sarcoplasmic reticulum, has been observed in a variety of muscle abnormalities [36], including muscular dystrophy [13,37,38]. Furthermore, it was recently shown by Malouf and Sommer [39] that many of these expanded membranes are continous with the extracellular space and probably originate from tubular structures. Our micrographs confirm these observations but also indicate that the dystrophic process is associated with a proliferation of junctional sarcoplasmic reticulum as well as tubular membranes. As a result, preparations of microsomes from dystrophic muscle yield a considerable number of elements presenting ultrastructural features similar to those of the proliferated junctional membranes in the whole muscle.

The protein to lipid ratio of dystrophic microsomes is markedly decreased, although their main protein component remains the Ca^{2+}sensitive ATPase coupled to Ca^{2+} transport. This "pump" protein is able to catalyze ATP hydrolysis and Ca^{2+} transport at normal rates. However, dystrophic microsomes have a lower capacity to retain transported calcium.

It is suggested that proliferation of such membranes in the junctional and tubular regions of the sarcomere accounts for the altered excitation-contraction coupling [3,5] and cable properties [40] of the dystrophic muscle. Our experiments do not indicate whether the membrane proliferation is a primary or secondary defect in the development of dystrophy.

Acknowledgements

We thank Betty Gallagher from the Department of Ophthalmology at the Stanford School of Medicine, Stanford University for preparing the thin sections, and the Electron Microscope Laboratory at the University of California in Berkeley for making the Balzers freeze fracturing device available to us. Appreciation is extended to Dr. B. Wilson and F. Lantz of the Department of Avian Sciences of the University of California, Davis, for supplying us with experimental animals. We also thank R.K. Smith and N. Kimura for their competent technical assistance. This work was supported by the National Institute of Health (HL 16607) and the Muscular Dystrophy Association of America. Dr. Sabbadini is a postdoctoral fellow supported by the Muscular Dystrophy Association.

References

1 Sandow, A. and Brust, M. (1958) Am. J. Physiol. 194, 557—563
2 Brust, M. (1965) Am. J. Physiol. 208, 431—435
3 Desmedt, J. (1967) in Exploratory Concepts of Muscular Dystrophy and Other Related Disorders (Milhorat, A.T., ed.), pp. 224—231, Excepta Med. Found., Amsterdam
4 Douglas, B. and Baskin, R.J. (1971) Am. J. Physiol. 220, 1344—1354
5 Sabbadini, R. and Baskin, R. (1976) Am. J. Physiol. 230, 1138—1147
6 Oppenheimer, H., Barany, K. and Milhorat, A.T. (1964) Proc. Soc. Exp. Bio. Med. 119, 877—880
7 Barany, M., Gaetjens, E. and Barany, K. (1966) 138, 360—366
8 Morey, K., Tarezy-Hornoch, K., Richards, E. and Brown, W. (1967) Arch. Biochem. Biophys. 119, 491—497
9 Kaldor, G. and Hsu, Q. (1975) Proc. Soc. Exp. Bio. Med. 149, 362—366
10 Dhalla, N., Singh, A., Lee, S., Anand, M., Bernatsky, A. and Jasmin, G. (1975) Clin Sci. Mol. Med. 49, 359—368
11 Sreter, F., Ikemoto, N. and Gergely, J. (1967) in Exploratory Concepts of Muscular Dystrophy and Related Disorders (Milhorat, A.T., ed.), pp. 289—298, Excerpta Med. Found., Amsterdam
12 Martonosi, A. (1968) Proc. Soc. Exp. Bio. Med., 127, 824—828
13 Baskin, R.J. (1970) Lab. Invest. 23, 581—589
14 Hsu, Q. and Kaldor, G. (1971) Proc. Soc. Exp. Bio. Med. 138, 733—737
15 Sylvester, R. and Baskin, R.J. (1973) Biochem. Med. 8, 213—227
16 Louis, C. and Irving, I. (1974) Biochim. Biophys. Acta 365, 193—202
17 Sabbadini, R., Scales, D. and Inesi, G. (1975) FEBS Lett. 54, 8—12
18 Peter, J. and Worsfold, M. (1969) Biochem. Med. 2, 364—371
19 Takagi, A., Schotland, D. and Rowland, L. (1973) Arch. Neurol. 28, 380—384
20 Sugita, H., Okimoto, K., Ebashi, S. and Okinaka, S. (1967), in Exploratory Concepts of Muscular Dystrophy and Related Disorders (Milhorat, A.T., ed.) pp. 321—326, Excerpta Med. Found., Amsterdam
21 Inesi, G. and Scales, D. (1974) Biochemistry 13, 3298—3306
22 Martonosi, A. and Feretos, R. (1964) J. Biol. Chem. 239, 648—657
23 Fiske, H. and Subbarow, Y. (1925) J. Biol. Chem. 66, 375—387

24 Tillack, T.W., Boland, R. and Martonosi, A. (1974) J. Biol. Chem. 249, 624—633
25 Martonosi, A. and Halpin, L.A. (1971) Arch. Biochem. Biophys. 144, 66—77
26 Meissner, G. and Fleischer, S. (1971) Biochim. Biophys. Acta 241, 356—378
27 MacLennan, D., Yip, C., Iles, G.H. and Seeman, P. (1972) in Cold Spring Harbor Symp. on Quantitative Biology, 37, 469—477
28 Inesi, G. and Asai, H. (1968) Arch. Biochem. Biophys. 126, 469—477
29 Ikemoto, N., Sreter, F.A., Nakamura, A. and Gergely, I. (1968) J. Ultrastruct. Res. 23, 216—232
30 Branton, D. (1966) Proc. Natl. Acad. Sci. U.S. 55, 1048
31 Deamer, D. and Baskin, R. (1969) J. Cell Biol. 42, 296—307
32 MacLennan, D., Seeman, P., Iles, G.H. and Yip, C. (1971) J. Biol. Chem. 246, 2702—2910
33 Scales, D. and Inesi, G. (1976) Biophys. J. 16, 735—751
34 Franzini-Armstrong, C. (1975) Fed. Proc. 34, 1382—1388
35 Hasselbach, W. and Makinose, M. (1961), Biochem. Z. 333, 518—528
36 Hudgson, P. and Pearce, G.W. (1969) in Disorders of Voluntary Muscle Walton, J.N., ed.), pp. 277—317, Little, Brown and Company, Boston
37 Van Breemen, V.L. (1960) Am. J. Path. 37, 333—336
38 Milhorat, A.T., Shafiq, S.A. and Goldstone, L. (1966) Ann. N.Y. Acad. Sci. 138, 246—292
39 Malouf, N. and Sommer, J. (1976) Am. J. Path. 84, 299—316
40 Lebeda, F. and Albuquerque, E. (1975) Exp. Neurol. 47, 544—557